Microbial Cell Factories

RESEARCH Open Access

Metabolic flux analysis of coenzyme Q_{10} synthesized by *Rhodobacter sphaeroides* under the influence of different pH regulators

Yujun Xiao[1†], Yi Zheng[1*†], Yong Zhou[1], Chaofan Yu[1] and Ting-E Ye[1]

Abstract

Coenzyme Q_{10} (CoQ_{10}) is crucial for human beings, especially in the fields of biology and medicine. The aim of this experiment was to investigate the conditions for increasing CoQ_{10} production. At present, microbial fermentation is the main production method of CoQ_{10}, and the production process of microbial CoQ_{10} metabolism control fermentation is very critical. Metabolic flux is one of the most important determinants of cell physiology in metabolic engineering. Metabolic flux analysis (MFA) is used to estimate the intracellular flux in metabolic networks. In this experiment, *Rhodobacter sphaeroides* was used as the research object to analyze the effects of aqueous ammonia ($NH_3{\cdot}H_2O$) and calcium carbonate ($CaCO_3$) on the metabolic flux of CoQ_{10}. When $CaCO_3$ was used to adjust the pH, the yield of CoQ_{10} was 274.43 $mg{\cdot}L^{-1}$ (8.71 $mg{\cdot}g^{-1}$ DCW), which was higher than that of $NH_3{\cdot}H_2O$ adjustment. The results indicated that when $CaCO_3$ was used to adjust pH, more glucose-6-phosphate (G6P) entered the pentose phosphate (HMP) pathway and produced more NADPH, which enhanced the synthesis of CoQ_{10}. At the chorismic acid node, more metabolic fluxes were involved in the synthesis of p-hydroxybenzoic acid (pHBA; the synthetic precursor of CoQ_{10}), enhancing the anabolic flow of CoQ_{10}. In addition, Ca^{2+} produced by the reaction of $CaCO_3$ with organic acids promotes the synthesis of CoQ_{10}. In summary, the use of $CaCO_3$ adjustment is more favorable for the synthesis of CoQ_{10} by *R. sphaeroides* than $NH_3{\cdot}H_2O$ adjustment. The migration of metabolic flux caused by the perturbation of culture conditions was analyzed to compare the changes in the distribution of intracellular metabolic fluxes for the synthesis of CoQ_{10}. Thus, the main nodes of the metabolic network were identified as G6P and chorismic acid. This provides a theoretical basis for the modification of genes related to the CoQ_{10} synthesis pathway.

Keywords CoQ_{10}, Metabolic flux, Metabolic engineering, *Rhodobacter sphaeroides*

†Yujun Xiao and Yi Zheng are co-first authors.

*Correspondence:
Yi Zheng
eyizheng@fjnu.edu.cn
[1]National Joint Engineering Research Center of Industrial Microbiology and Fermentation Technology, College of Life Sciences, Fujian Normal University, Fuzhou, China

Introduction

Coenzyme Q_n (CoQ_n) is a lipid-soluble quinone compound formed by conjugation of the benzoquinone group at the head and a polyisoprene hydrophobic side chain at the tail [1]. It exists in the cells of various organisms. The subscript n of CoQ_n represents the number of isoprene repeating units in the molecule. The number of isoprene units on the side chains of CoQ_n varies from organism to organism. The CoQ_n molecule in the human body contains 10 isoprene units, namely CoQ_{10}. CoQ_{10} was discovered by Frederick Crane and colleagues in 1957 [2]. CoQ_{10} is the only lipid-soluble antioxidant synthesized endogenously in the human body [3]. Reduced CoQ_{10} (Fig. 1) is the main form present in the body, accounting for more than 90% of the total CoQ_{10} in the human circulation [4, 5]. The reduced CoQ_{10} releases electrons during the electron transfer process, and the electrons are transferred through the respiratory chain to eventually produce ATP to provide energy for the body. CoQ_{10} deficiency in the human body will cause some diseases. In addition, CoQ_{10} is also beneficial to the skin. It can improve the skin and enhance the expression of collagen and elastin [6, 7]. It has been shown that CoQ_{10} levels in skin and skin surface lipids decline with age. CoQ_{10} is very important to human beings and has great value. It is used in many fields such as medicine, food, and cosmetics.

There are three main methods to produce CoQ_{10}. However, there is a preference for the microbial fermentation method, which is considered the most feasible, over the biological tissue extraction method and chemical synthesis method [8–10]. CoQ_{10} synthesized by microbial fermentation is an all-trans conformation with biological activity, and the method does not produce other optical isomers [11, 12]. In addition, microorganisms grow and reproduce quickly, can utilize inexpensive raw materials, and produce fewer contaminants during the production process. One of the microorganisms that can synthesize CoQ_{10} efficiently and has been used in industrial production is *Rhodobacter sphaeroides* [13, 14]. It is a gram-negative purple non sulfur bacterium (PNSB) that can grow aerobically, anaerobically, photoautotrophically, and heterotrophically [15–17]. It has many other functions, such as biological hydrogen production, synthesis of carotenoids, fixation of CO_2 and N_2, remediation of heavy metal pollution and power generation [18–21].

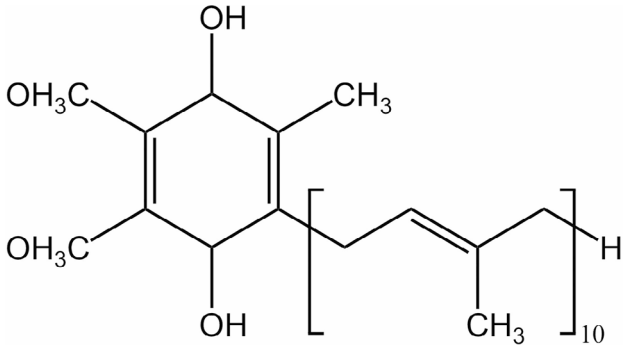

Fig. 1 Chemical structure of reduced CoQ_{10} ($CoQ_{10}H_2$)

Extracellular organic acids are continuously produced by *R. sphaeroides* during the fermentation of CoQ_{10}. This leads to a continuous decrease in the pH of the environment and affects the physiological activity of the bacteria. Organic acids are generally neutralized by adding $CaCO_3$ or $NH_3{\cdot}H_2O$.

The process of CoQ_{10} biosynthesis in *R. sphaeroides* is complex (Fig. 2). First, the head quinone ring and the tail polyisoprene chain of CoQ_{10} need to be synthesized separately [22]. The synthesis of the quinone ring is the shikimate pathway. This pathway uses erythrose-4-phosphate (E4P) and phosphoenolpyruvate (PEP) as the starting substrates, which are converted to chorismic acid in various steps. The chorismic acid is then converted to p-hydroxybenzoic acid (pHBA), a precursor of the quinone ring, by the action of the chorismic acid lyase encoded by the UbiC gene. The polyisoprene chain is synthesized via the methylerythritol phosphate (MEP) pathway. The starting substances of this pathway are glyceraldehyde-3-phosphate and pyruvate, which are converted to isopentenyl diphosphate (IPP) and dimethylallyl diphosphate (DMAPP) by various reactions, and then formed into decaprenyl diphosphate (DPP) by various reactions. DPP and pHBA are converted to 3-decaprenyl-4-hydroxybenzoate via the ubiquinone pathway by the action of p-hydroxybenzoic acid polyisoprene transferase encoded by the UbiA gene and enter the quinone ring modification pathway. After decarboxylation, hydroxylation, and methylation processes, CoQ_{10} is finally formed.

Methods and materials

Microorganism and culture media

The *R. sphaeroides* used in this study was the F3-40 strain (from the College of Life Sciences, Fujian Normal University, Fuzhou, China). The culture media included agar slant culture medium (containing 18 $g{\cdot}L^{-1}$ glucose, 4.5 $g{\cdot}L^{-1}$ yeast powder, 20 $g{\cdot}L^{-1}$ agar powder, 2 $g{\cdot}L^{-1}$ monosodium glutamate, 5.25 $g{\cdot}L^{-1}$ $(NH_4)_2SO_4$, 4.2 $g{\cdot}L^{-1}$ NaCl, 8.75 $g{\cdot}L^{-1}$ $MgSO_4$, 1.5 $g{\cdot}L^{-1}$ KH_2PO_4, 1.2 $g{\cdot}L^{-1}$ A), seed culture medium (containing 18 $g{\cdot}L^{-1}$ glucose, 4.5 $g{\cdot}L^{-1}$ yeast powder, 2 $g{\cdot}L^{-1}$ monosodium glutamate, 5.25 $g{\cdot}L^{-1}$ $(NH_4)_2SO_4$, 4.2 $g{\cdot}L^{-1}$ NaCl, 8.75 $g{\cdot}L^{-1}$ $MgSO_4$, 1.5 $g{\cdot}L^{-1}$ KH_2PO_4, 1.2 $g{\cdot}L^{-1}$ A), and fermentation culture medium (containing 35.6 $g{\cdot}L^{-1}$ glucose, 6.39 $g{\cdot}L^{-1}$ corn steep powder, 7.39 $g{\cdot}L^{-1}$ monosodium glutamate, 6.28 $g{\cdot}L^{-1}$ $(NH_4)_2SO_4$, 2.5 $g{\cdot}L^{-1}$ NaCl, 12 $g{\cdot}L^{-1}$ $MgSO_4$, 0.8 $g{\cdot}L^{-1}$ KH_2PO_4, 0.1 $g{\cdot}L^{-1}$ $MnSO_4$, 1.6 $g{\cdot}L^{-1}$ A, 0.1 $g{\cdot}L^{-1}$ B).

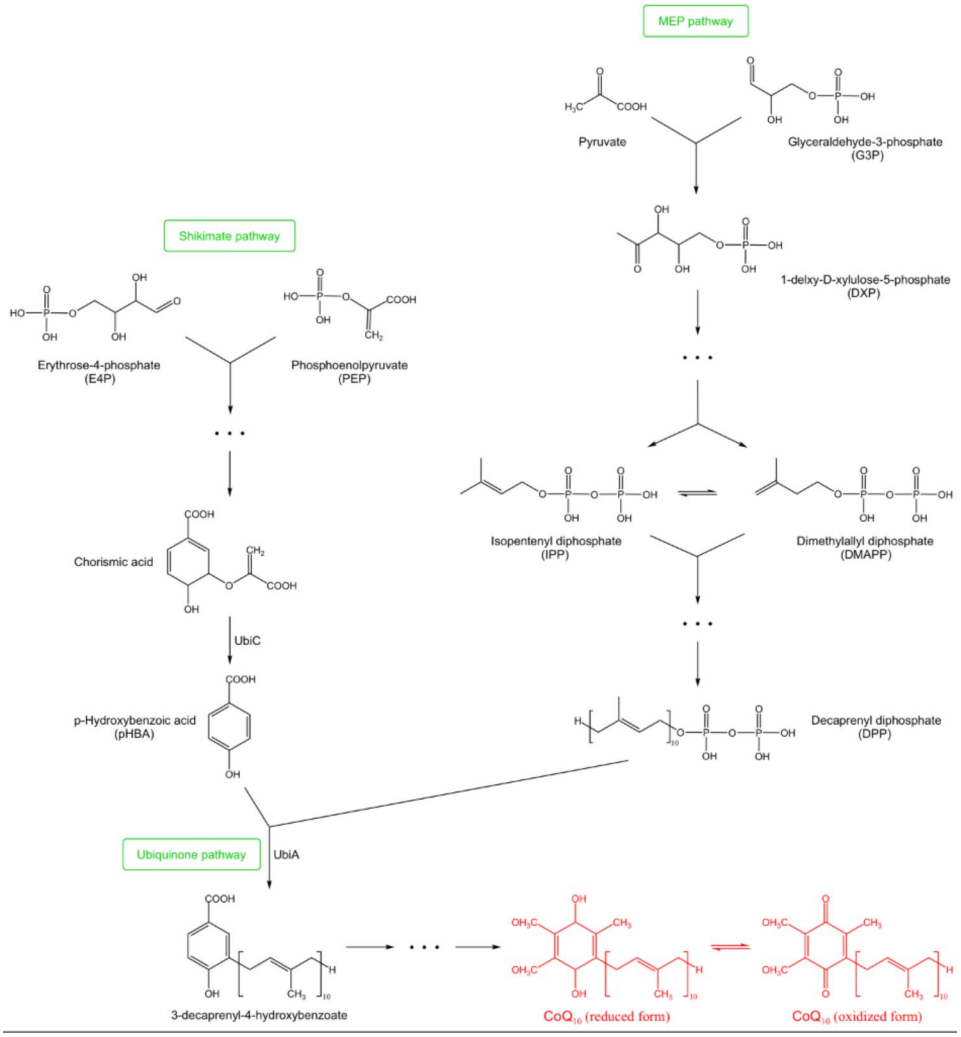

Fig. 2 CoQ_{10} synthesis pathway in *R. sphaeroides*

Cultivation method

Two colonies of *R. sphaeroides* cultured on agar plates for 6 days were picked out and transferred into the primary seed medium (50 mL/250 mL), and incubated at 32 °C with shaking at 220 rpm for 24 h. Then, they were transferred into the secondary seed medium (350 mL/2500 mL) at 10% inoculum and incubated at 32 °C with shaking at 220 rpm for 22 h. Finally, the secondary seed medium was inoculated at 15% inoculum into a 10 L fermenter. The inoculated fermenter was filled with 7 L. The temperature was 34 °C, the stirring speed was 300 rpm, the aeration rate was 3 $L{\cdot}min^{-1}$, and the tank pressure was 0.04 MPa. The pH was adjusted by adding $CaCO_3$ and $NH_3{\cdot}H_2O$ during the fermentation process. Samples were taken at 3 h intervals to determine various parameters.

Determination of glucose

A bioanalytical sensor (model SBA-40D, from Biology Institute of Shandong Academy of Sciences) was used for analysis. The fermentation broth was diluted by a certain multiple and then filtered. Twenty-five microliters of filtrate was taken for injection determination. The determination was performed three times in parallel and the average value was taken.

Determination of cell dry weight (DCW)

Five milliliters of the fermentation broth was centrifuged (1×10^4 rpm, 10 min), and the supernatant was removed. After washing with distilled water, the samples were centrifuged again, and the supernatant was removed. The organism in the centrifuge tube was dried in an oven at 100 °C to a constant weight. For fermentation broth containing $CaCO_3$, a drop of 6 $mol{\cdot}L^{-1}$ HCl solution was added to dissolve the residual $CaCO_3$ in the fermentation broth before centrifugation.

Extraction of CoQ_{10} and determination of its content

CoQ_{10} was extracted by ultrasonic extraction [23, 24]. Five milliliters of the fermentation broth was added to a 50 mL brown volumetric flask. A drop of 6 mol·L^{-1} HCl solution was added. Shake well and add 10 mL of acetone. After mixing, 0.5 mL of 30% H_2O_2 solution was added. Finally, 20–30 mL ethanol was added. The volumetric flask was placed into the ultrasonic cleaner for 1 min, and the volumetric flask was not capped. Subsequently, the volumetric flask was fixed with ethanol and capped. A strip of cardboard was used to separate the cap from the neck of the bottle to retain the gap. The volumetric flask was again placed in an ultrasonic cleaner for 45 min, with the temperature controlled below 35 °C. At the end of the treatment, the flask was well shaken and allowed to stand for 30 min. Finally, the supernatant was filtered through a 0.22 μm organic filter.

The filtrate was collected for the determination of CoQ_{10} by high-performance liquid chromatography (HPLC). The chromatographic column was Hypersil ODS-SP (4.6 mm × 100 mm, 5 μm). The mobile phase consisted of anhydrous methanol and anhydrous ethanol in a ratio of 65: 35 (v/v). The detection wavelength was set at 275 nm. The column temperature was 30 °C, the injection volume was 20 μL, the flow rate was 1.1 mL·min^{-1}, and the elution time was 15 min. The calculation formula of CoQ_{10} concentration in the sample is:

$$c = \frac{S \cdot V_o \cdot K \cdot c_o}{S_o \cdot V}$$

where c is the concentration of CoQ_{10} in the test sample (mg·L^{-1}); c_o is the concentration of CoQ_{10} in the standard sample (mg·L^{-1}); K is the dilution multiple of the test sample; S is the peak area of the test sample (mAU·s); S_o is the peak area of the standard sample (mAU·s); V is the injection volume of the test sample (μL); and V_o is the injection volume of the standard sample (μL).

Table 1 Distribution of cellular fraction components of *R. sphaeroides* under aerobic contributions

Component	Content (mmol·g^{-1} DCW)	Component	Content (mmol·g^{-1} DCW)	Component	Content (mmol·g^{-1} DCW)
Ala	0.8189	Lys	0.1669	CTP	0.0904
Arg	0.431	Met	0.1585	UTP	0.0436
Asn	0.1423	Phe	0.2041	dATP	0.0185
Asp	0.3344	Pro	0.3242	dTTP	0.0186
Cys	0.0714	Ser	0.2738	dGTP	0.0412
Gln	0.1603	Thr	0.3134	dCTP	0.0415
Glu	0.401	Trp	0.063	PE	0.077
Gly	0.5535	Tyr	0.1207	PG	0.0867
His	0.1363	Val	0.4527	PC	0.0385
Ile	0.2906	ATP	0.0455	DPG	0.0024
Leu	0.5511	GTP	0.0932	SQDG	0.0241

Determination of various free amino acid concentrations

The concentration of free amino acids in the fermentation broth was determined by HPLC. A Venusil-AA amino acid analysis column was used. Mobile phases A and B were 0.1 mol·L^{-1} CH_3COONa solution (pH 6.5) and 80% acetonitrile solution, respectively. The detection wavelength was set at 254 nm. The column temperature was 40 °C, the injection volume was 20 μL, and the flow rate was 1 ml·min^{-1}. Gradient elution was performed.

Determination of organic acid concentration

The concentration of organic acids in the fermentation broth was determined by HPLC [25]. The chromatographic column was an Inertsil ODS-SP C18. Mobile phases A and B were 0.01 mol·L^{-1} KH_2PO_4 buffer (pH adjusted to 2.8 by H_3PO_4) and acetonitrile solution, respectively, and were injected into the column at a ratio of 95: 5 (v/v). The detection wavelength was set at 215 nm. The column temperature was 25 °C, the injection volume was 20 μL, and the flow rate was 1 ml·min^{-1}.

Results

Construction of a metabolic network for CoQ_{10} synthesis in *R. sphaeroides*

The synthesis of CoQ_{10} by *R. sphaeroides* belongs to growth-coupled fermentation. Therefore, when analyzing the metabolic flux of CoQ_{10} synthesis, the carbon source consumed by the growth of the bacterium cannot be ignored, and the synthesis pathway of the basic cellular components should be considered. The main cellular components and their contents refer to the experimental data measured by Saheed lmam [26]. The fractions of *R. sphaeroides* under aerobic conditions are shown in Table 1. It contained 17.6% pHBA. Among fatty acids, oleic acid (C_{18}:1) has the highest content, accounting for 85%. Stearic acid (C_{18}:0), soft fatty acid (C_{16}:0), and palmitoleic acid (C_{16}:1) accounted for 9%, 5%, and 1%, respectively.

Since *R. sphaeroides* uses glucose as the sole carbon source, the glyoxylate cycle pathway is largely inoperative and is not considered in this metabolic network. The intermediate reactions without branching points are simplified into a reaction equation. For intermediate metabolites with branching points, the rate of production was equal to the rate of consumption, and the net accumulation was 0, assuming that these metabolites were in the proposed steady state.

It is assumed that NADPH produced by the HMP pathway and the TCA pathway were not oxidatively phosphorylated but were all used for biosynthesis. The fermentation supernatant of 39–42 h in the late logarithmic growth phase of the organism was analyzed for composition. The results showed that the supernatant basically did not contain free amino acids. The content of

organic acid metabolic byproducts such as formic acid, acetic acid, propionic acid, butyric acid, lactic acid, pyruvic acid, and citric acid was also very low. Therefore, the influence of these organic acids on metabolic flux can be ignored in the metabolic network studied.

Modeling of metabolic flux equilibrium for CoQ_{10} synthesis by *R. sphaeroides*

Metabolic flux analysis is a metabolic network chemometric used to describe the conversion of substrates into metabolites and cellular composition. The distribution of carbon flow under the condition of carbon source limitation is generally considered. The equilibrium equation of each metabolite can be expressed as:

$$\frac{dX_{met}}{dt} = r_{met} - uX_{met}$$

where X_{met} is the metabolite concentration; r_{met} is the net rate of metabolite formation; and u is the dilution factor of the culture medium.

Since most of the intermediate metabolites have low intracellular concentrations, the dilution effect can be negligible. According to the proposed steady-state assumption that the concentration of intermediate metabolites is in equilibrium ($dX_{met}/dt=0$), it follows that: $r_{met} = 0$.

The net rate of intermediate metabolite formation used is expressed in the form of a matrix equation as:

$$S \cdot v = 0$$

where S is the n × m stoichiometric coefficient matrix, and the rows of the matrix represent the stoichiometric coefficients of the rate reactions of the intermediate metabolites; v is an m-dimensional column vector; n is the number of intermediate metabolites; and m is the total number of metabolic reaction rates.

The degree of freedom to be solved is F=m - n. The number of linearly uncorrelated rates is determined experimentally. The matrix equation $S \cdot v=0$ has a unique solution as long as it is greater than or equal to the degree of freedom F. Then, the undetermined metabolic reaction rates can be calculated, and thus, the flux distribution of the metabolic network can be determined.

Based on the intracellular composition and biosynthetic analysis of the various metabolites in the metabolic network, the following proposed steady-state equilibrium equation of the branch point intermediates was obtained:

G6P: r_1-r_2-r_{10}-r_{11}-$0.0241r_{21}$=0.
F6P: r_2-r_3+$0.6667r_{13}$+r_{14}=0.
Ru5P: r_{11}-$0.5288r_{12}$-r_{13}-$2r_{14}$-$0.063r_{15}$=0.
GA3P: $2r_3$-r_4+$0.3333r_{13}$+$0.063r_{15}$-$10r_{16}$-$0.313r_{21}$=0.
PG: r_4-r_5-$0.1984r_{12}$-$0.8987r_{20}$-$0.1155r_{21}$=0.
PEP: r_5-r_6-$2r_{14}$-$0.063r_{15}$=0.
Pyr: r_6-r_7+$0.063r_{15}$-$9r_{16}$-$2.0895r_{17}$-r_{18}-$0.4575r_{19}$=0.
AcCoA: r_7-r_8-$0.5511r_{17}$-$8.0862r_{21}$=0.
OAA: -r_8+r_9-$0.1941r_{12}$+r_{18}-$1.4061r_{19}$=0.
Chr: r_{14}-$0.3878r_{15}$-r_{16}=0.
AKG: r_8-r_9-$1.3165r_{22}$=0.
NADPH: r_8+$2r_{11}$-$0.911r_{12}$-r_{14}-$0.3878r_{15}$-$10r_{16}$-$2.0895r_{17}$-$4.8055r_{19}$-$1.1843r_{20}$-$7.3028r_{21}$-$3.2579r_{22}$=0.

When these equilibrium equations were constructed into a matrix equation, the rank of the matrix n=12 was calculated. If the unknown rate variable J=22, then the matrix has degrees of freedom F=J - n=10. If the matrix equation is to have a unique solution, at least 10 rate variables must be determined. Of these 22 rate variables, r_{10}, r_{12}, r_{15}, r_{17}, r_{19}, r_{20}, r_{21}, and r_{22} were calculated by measuring the synthesis rate of cell dry weight. Through the sugar consumption rate, r_1 can be obtained. Through the synthesis rate of CoQ_{10}, r_{16} can be obtained. From the data of these 10 rate variables, the remaining 12 unknown rate variables can be calculated using MATLAB software.

Analysis of the effects of two pH regulators on the synthetic metabolic flux of CoQ_{10}

The synthesis rate of CoQ_{10} was significantly higher in the late logarithmic growth phase than in the mid and early growth periods when the pH was adjusted by $CaCO_3$ or $NH_3{\cdot}H_2O$. Then, metabolic flux analysis was performed to quantify the flux distribution of the CoQ_{10} synthesis pathway in the late logarithmic growth phase of these two fermentations. Flux analysis was performed using the 42nd hour of fermentation as the time point. The variable rates of metabolites (r_1 to r_{22}) were divided by the rate of glucose consumption (r_1), and the result was the respective values of r1 to r22 (Table 2).

$$C = \frac{Flux\,(CaCO_3 adjustment) - Flux(NH_3 \cdot H_2O adjustment)}{Flux(NH_3 \cdot H_2O adjustment)}$$

It can be seen from Fig. 3 and Table 2 that the two pH regulators caused significant changes in the flux distribution of G6P, Ru5P, and PEP nodes. The values of r2 to r9 on the EMP pathway and TCA pathway were smaller, while the values of r11 and r13 on the HMP pathway were larger when $CaCO_3$ was used to adjust pH compared to $NH_3{\cdot}H_2O$. This indicates that $CaCO_3$ adjustment strengthened the HMP pathway and weakened the EMP pathway and TCA pathway.

The change in r16 showed that the metabolic flux from Chr to CoQ_{10} under $CaCO_3$ adjustment was 0.13, while $NH_3{\cdot}H_2O$ adjustment resulted in 0.03. The enhanced metabolic flux from Chr to CoQ_{10} increased the demand for NADPH, prompting more G6P to flow into the HMP pathway to form NADPH. However, $CaCO_3$ adjustment has little effect on biosynthesis. Thus, the increased portion of

Table 2 The metabolic flux distribution of CoQ_{10} under different pH adjustment modes

Flux	$CaCO_3$ adjustment	$NH_3{\cdot}H_2O$ adjustment	C (%)
r1	100	100	0
r2	27.88	30.45	-8.44
r3	73.56	74.46	-1.21
r4	82.62	83.42	-0.96
r5	79.56	80.38	-1.02
r6	78.63	79.51	-1.11
r7	60.73	62	-2.05
r8	8.06	9.15	-11.91
r9	12.6	15.37	-18.02
r10	1.29	1.28	0.78
r11	70.54	67.99	3.75
r12	1.22	1.21	0.83
r13	56.02	54.01	3.72
r14	1.44	1.33	8.27
r15	1.31	1.3	0.77
r16	0.13	0.03	333.33
r17	5.94	5.9	0.68
r18	9.99	9.91	0.81
r19	6.9	6.85	0.73
r20	2.12	2.1	0.95
r21	31.37	31.15	0.7
r22	7.57	7.51	0.80

G6P entering the HMP pathway was not used for the synthesis of bacterial cells, but formed G6P and GA3P and returned to the EMP pathway for oxidative catabolism in the TCA pathway.

The organic acids produced during fermentation react with $CaCO_3$ to form Ca^{2+}, which activates enzymes related to the CoQ_{10} synthesis pathway and stimulates the production of reactive oxygen species (ROS) that can damage cell membranes [27]. Since CoQ_{10} has antioxidant properties, it can alleviate the damage caused by ROS on cell membranes. With the increase in Ca^{2+} concentration, the formation of intracellular ROS was stimulated, which promoted the synthesis of CoQ_{10} and increased the yield of CoQ_{10}.

A certain amount of Ca^{2+} has been proven to increase the yield of CoQ_{10}. Whether different concentrations of Ca^{2+} can all achieve this effect is an aspect worthy of future research, and perhaps the best Ca^{2+} concentration can be found. Ca^{2+} is an activator of many enzymes, and the hypothesis that increased CoQ_{10} yield may also be due to its activation of the activity of related enzymes in the synthesis pathway can also be explored.

Changes in metabolic flux in G6P and Ru5P nodes

G6P is the common starting metabolite of both the EMP pathway and the HMP pathway. When $CaCO_3$ was used to adjust the pH, the metabolic flux from G6P to Ru5P was 70.5, and the metabolic flux from G6P to F6P was 27.9 (Fig. 4). When $NH_3{\cdot}H_2O$ was used to adjust the pH, the metabolic flux from G6P to Ru5P was 68, and the metabolic flux from G6P to F6P was 30.4. The difference in metabolic flux caused by these two pH adjustment methods was equal between G6P to Ru5P and G6P to F6P. However, the increased metabolic flux of Ru5P had almost no effect on nucleic acid and histidine synthesis in the bacterium, which was mostly converted to F6P and GA3P (approximately 2.01). The metabolic flux from G6P to F6P migrates due to the addition of $CaCO_3$ during fermentation or the effect of the reduction of NH_4^+ on fermentation. Some of the metabolic streams passed through the HMP pathway before entering the EMP pathway. This process has a completely different meaning than that of F6P, which is directly converted to F6P by the EMP pathway. Although the loss of carbon source material flux is small, the former provides more reducing power NADPH. Since the synthesis of isoprene pyrophosphate, the precursor of the CoQ_{10} side chain, requires NADPH to provide reducing power, 10 mol NADPH is directly involved for every 1 mol CoQ_{10} synthesis. Then, G6P enters the EMP pathway through the HMP pathway to provide NADPH for the synthesis of CoQ_{10}.

Analysis of the effects of two pH regulators on the synthesis of CoQ_{10} by *R. sphaeroides*

The two pH regulators, $CaCO_3$ and $NH_3{\cdot}H_2O$, had almost no effect on the biosynthesis of the bacterium during the synthesis of CoQ_{10} by *R. sphaeroides*. The fermentation times used for conditioning with $CaCO_3$ and $NH_3{\cdot}H_2O$ were 50 h and 45 h, respectively (Table 3). The difference in CoQ_{10} yield caused by the two pH regulators was significant (Fig. 5). When the fermentation endpoint was reached, the CoQ_{10} yield with $CaCO_3$ conditioning was 274.43 $mg{\cdot}L^{-1}$ (8.71 $mg{\cdot}g^{-1}$ DCW), which was higher than that of $NH_3{\cdot}H_2O$ conditioning of 226.53 $mg{\cdot}L^{-1}$ (7.55 $mg{\cdot}g^{-1}$ DCW). The CoQ_{10} synthesis rates under the two pH adjustments were basically the same within 24 h from the beginning of fermentation. However, between 24 and 42 h, the rate of CoQ_{10} synthesis under $NH_3{\cdot}H_2O$ regulation was faster than that under $CaCO_3$ regulation. The accelerated synthesis of CoQ_{10} in this process produces more organic acids. As an alkaline substance, $NH_3{\cdot}H_2O$ with high solubility can quickly resist the pH drop caused by organic acids, while $CaCO_3$ with poor solubility reacts slowly. Therefore, $NH_3{\cdot}H_2O$ can better regulate the pH in this stage, which leads to a faster rate of CoQ_{10} synthesis. After 42 h of fermentation, the rate of $NH_3{\cdot}H_2O$-regulated CoQ_{10} synthesis slowed down, whereas the $CaCO_3$-regulated one was still able to maintain a high rate of growth. The reason was mainly that $NH_3{\cdot}H_2O$ was consumed in large quantities in the early stage, the concentration decreased dramatically, and the pH-regulating ability was weakened.

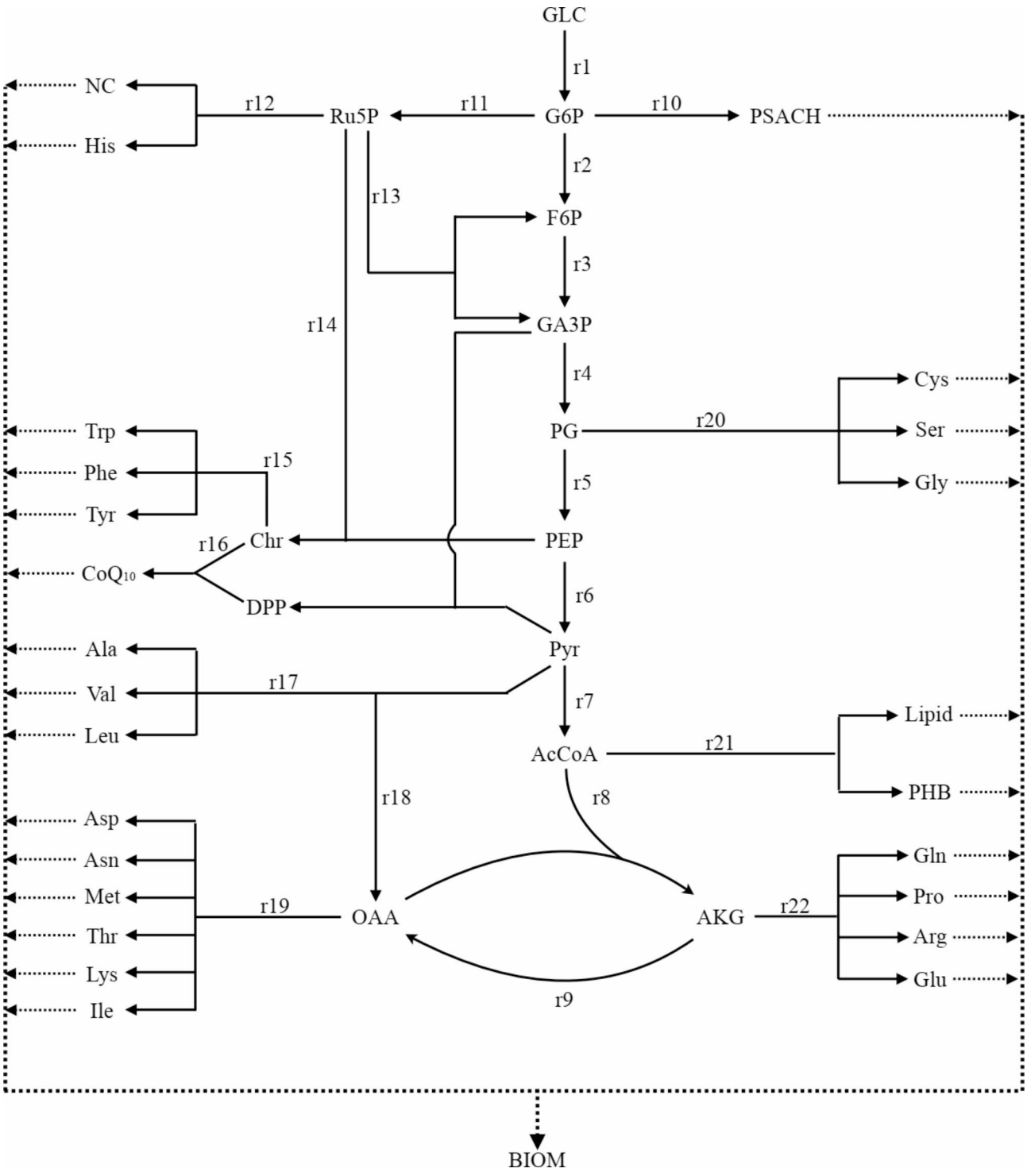

Fig. 3 Metabolic network of CoQ_{10} synthesis in *R. sphaeroides.* AcCoA (Acetyl coenzyme A); AKG (a-Ketoglutarate); BIOM (biomass); Chr (Chorismate); F6P (Fructose-6-phosphate); G6P (Glucose-6-phosphate); GA3P (Glyceraldehyde-3-phosphate); GLC (Glucose); OAA (Oxaloacetate); PEP (Phosphoenolpyruvate); PG (3-Phosphoglycerate); PHB (poly-β-hydroxybutyrate); PSACH (Polysaccharides); PYR (Pyruvate); Ru5P (Ribulose-5-phosphate); NC (Nucleic Acids)

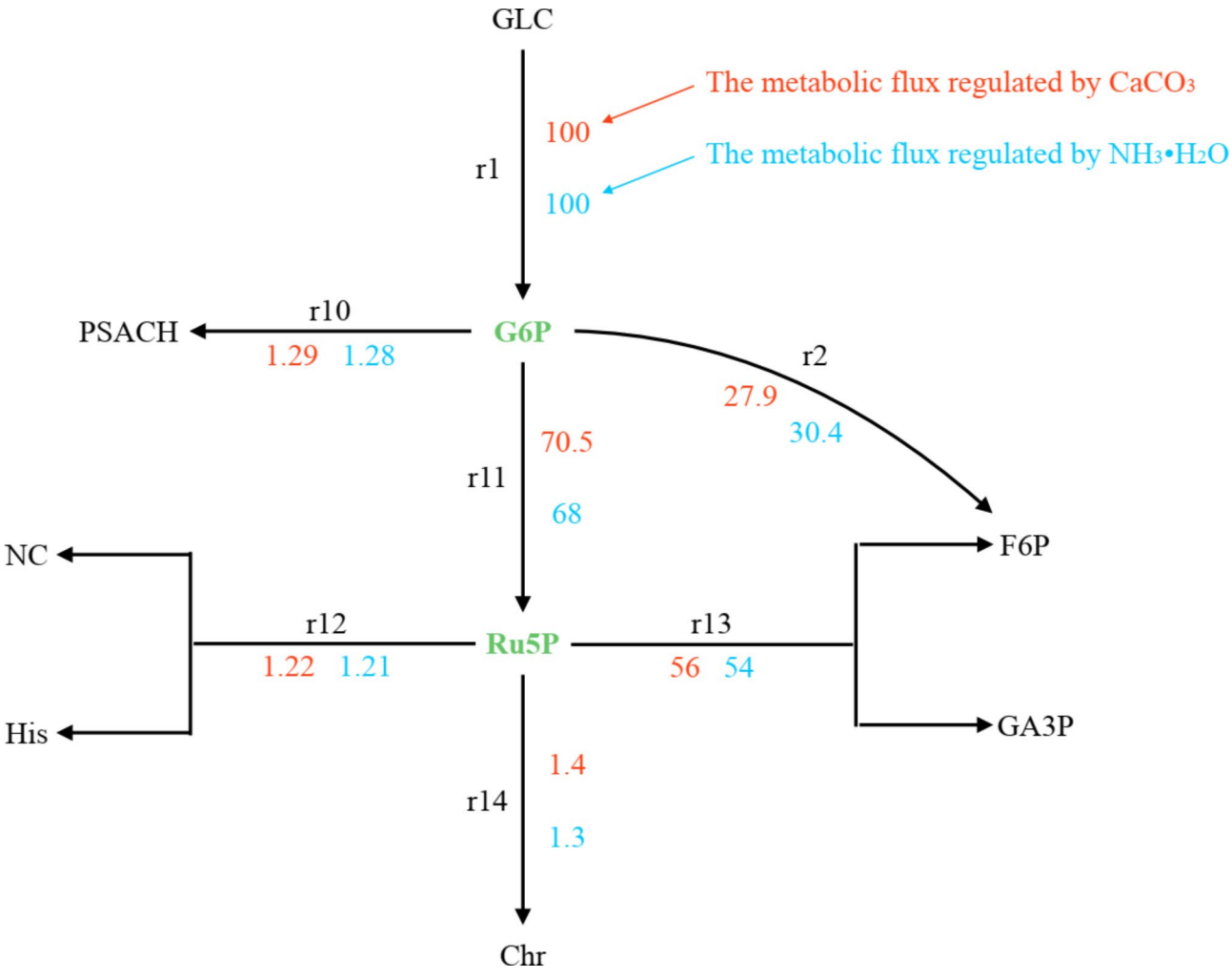

Fig. 4 The metabolic flux distribution of G6P and Ru5P nodes under different pH adjustment modes

Table 3 Comparison of various parameters of the fermentation process under two pH adjustment methods

Parameters	$CaCO_3$ adjustment	$NH_3{\cdot}H_2O$ adjustment
Initial glucose concentration ($g{\cdot}L^{-1}$)	31.5	30
Fermentation time (h)	50	45
The yield of CoQ_{10} ($mg{\cdot}L^{-1}$)	274.43	226.53
($mg{\cdot}g^{-1}$ DCW)	8.71	7.55
The specific generation rate of CoQ_{10} ($mg{\cdot}g^{-1}{\cdot}h^{-1}$)	0.3681	0.3323
Glucose consumption rate ($g{\cdot}L^{-1}{\cdot}h^{-1}$)	0.63	0.67
Glucose ratio consumption rate (h^{-1})	0.0439	0.0466
Production intensity ($mg{\cdot}L^{-1}{\cdot}h^{-1}$)	5.49	5.03
Average specific growth rate (h^{-1})	0.0242	0.0250
Maximum cell dry weight ($g{\cdot}L^{-1}$)	19.57	20.72

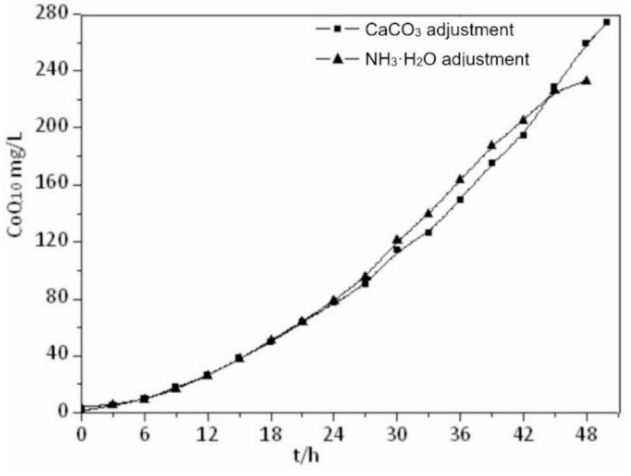

Fig. 5 Effects of two pH regulators on the yield of CoQ_{10}

Conclusions and future perspectives

In summary, pH adjustment with $CaCO_3$ was more favorable for the synthesis of CoQ_{10} by *R. sphaeroides* compared with $NH_3{\cdot}H_2O$ adjustment. This study provides a reference for researchers in the selection of pH regulators. In addition,

the main nodes of the metabolic network were identified as G6P and chorismic acid. This provides a theoretical basis for the modification of genes related to the CoQ_{10} synthesis pathway.

Due to the high value of CoQ_{10}, an increasing number of researchers are investigating it. Its potential functions are constantly being developed and explored. Microbial fermentation as a production method will be the choice of more people in the future, and one of its most important goals is to maximize the yield of the desired fermentation product. The method is not only the well-known improvement and selection of strains, but also the analysis of the culture environment favorable to the synthesis of products according to the metabolic network of the microorganism, as used in this article. The application of metabolic engineering principles to improve the yield of microbial fermentation products has become a hot research topic.

Authors' contributions
Yujun Xiao and Yi Zheng wrote the manuscript and analyzed the results. Yong Zhou performed the experiments and analyzed the results. Chaofan Yu and Ting-E Ye supervised the research. All authors have read and approved the final manuscript.

Funding
This work was supported by the Natural Science Foundation of Fujian Province, China (Grant Number 2015J01127).

Declarations

Competing interests
The authors declare no competing interests.

Ethics approval and consent to participate
Not applicable.

Consent for publication
Not applicable.

Received: 12 June 2023 / Accepted: 19 September 2023

References

1. Liu J, Wu Q, He D, Ma T, Du L, Dui W, Guo X, Jiao R. Drosophila sbo regulates lifespan through its function in the synthesis of coenzyme Q in vivo. J Genet Genomics. 2011;38(6):225–34.
2. Raizner AE, Quiñones MA. Coenzyme Q_{10} for Patients with Cardiovascular Disease: JACC Focus Seminar. J Am Coll Cardiol. 2021;77(5):609–19.
3. Bentinger M, Tekle M, Dallner G. Coenzyme Q–biosynthesis and functions. Biochem Biophys Res Commun. 2010;396(1):74–9.
4. Kuriyama N, Nakamura T, Nakazawa H, Wen T, Berra L, Bittner EA, Goverman J, Kaneki M. Bioavailability of reduced Coenzyme Q10 (Ubiquinol-10) in burn patients. Metabolites. 2022;12(7):613.
5. Ruiz-Jiménez J, Priego-Capote F, Mata-Granados JM, Quesada JM, Luque de Castro MD. Determination of the ubiquinol-10 and ubiquinone-10 (coenzyme Q10) in human serum by liquid chromatography tandem mass spectrometry to evaluate the oxidative stress. J Chromatogr. 2007;1175(2):242–8.
6. Vollmer DL, West VA, Lephart ED. Enhancing skin health: by oral administration of natural Compounds and Minerals with Implications to the dermal Microbiome. Int J Mol Sci. 2018;19(10):3059.
7. Žmitek K, Pogačnik T, Mervic L, Žmitek J, Pravst I. The effect of dietary intake of coenzyme Q10 on skin parameters and condition: results of a randomised, placebo-controlled, double-blind study. Biofactors. 2017;43(1):132–40.
8. Tian Y, Yue T, Yuan Y, Soma PK, Lo YM. Improvement of cultivation medium for enhanced production of coenzyme Q10 by photosynthetic *Rhodospirillum rubrum*. Biochem Eng J. 2010;51(3):160–6.
9. Tian Y, Yue T, Yuan Y, Soma PK, Williams PD, Machado PA, Fu H, Kratochvil RJ, Wei CI, Lo YM. Tobacco biomass hydrolysate enhances coenzyme Q10 production using photosynthetic *Rhodospirillum rubrum*. Bioresour Technol. 2010;101(20):7877–81.
10. Wang Y, Chen S, Liu J, Lv P, Cai D, Zhao G. Efficient production of coenzyme Q_{10} from acid hydrolysate of sweet sorghum juice by *Rhodobacter sphaeroides*. RSC Adv. 2019;9(39):22336–42.
11. Fan J, Xu W, Xu X, Wang Y. Production of Coenzyme Q10 by microbes: an update. World J Microbiol Biotechnol. 2022;38(11):194.
12. Lee SQ, Tan TS, Kawamukai M, Chen ES. Cellular factories for coenzyme Q_{10} production. Microb Cell Fact. 2017;16(1):39.
13. Yang Y, Li L, Sun H, Li Z, Qi Z, Liu X. Improving CoQ_{10} productivity by strengthening glucose transmembrane of *Rhodobacter sphaeroides*. Microb Cell Fact. 2021;20(1):207.
14. Zhang J, Gao D, Jiajia C, Liu H, Qi Z. Improving coenzyme Q_{10} yield of *Rhodobacter sphaeroides* via modifying redox respiration chain. Biochem Eng J. 2018;135:98–104.
15. Lee S, Yu J, Kim YH, Min J. Optimized *Rhodobacter sphaeroides* for the production of Antioxidants and the pigments with antioxidant activity. Mol Biotechnol. 2022;65(1):131–5.
16. Peng L, Lou W, Xu Y, Yu S, Liang C, Alloul A, Song K, Vlaeminck SE. Regulating light, oxygen and volatile fatty acids to boost the productivity of purple bacteria biomass, protein and co-enzyme Q10. Sci Total Environ. 2022;822:153489.
17. Yu J, Moon SK, Kim YH, Min J. Isoprene production by *Rhodobacter sphaeroides* and its antimicrobial activity. Res Microbiol. 2022;173:103938.
18. Cadirci BH. An electricity production study by *Rhodobacter sphaeroides*. Int J Hydrog Energy. 2018;43(38):18001–6.
19. Giotta L, Agostiano A, Italiano F, Milano F, Trotta M. Heavy metal ion influence on the photosynthetic growth of *Rhodobacter sphaeroides*. Chemosphere. 2006;62(9):1490–9.
20. Imam S, Noguera DR, Donohue TJ. Global insights into energetic and metabolic networks in *Rhodobacter sphaeroides*. BMC Syst Biol. 2013;7(1):89.
21. Liu S, Zhang G, Li X, Wu P, Zhang J. Enhancement of *Rhodobacter sphaeroides* growth and carotenoid production through biostimulation. J Environ Sci. 2015;33:21–8.
22. He S, Lu H, Zhang G, Ren Z. Production of coenzyme Q10 by purple non-sulfur bacteria: current development and future prospect. J Clean Prod. 2021;307:127326.
23. Wang Y, Fan L, Huang J, Liang J, Wang X, Ren Y, Li H, Yue T, Gao Z. Evaluation of chemical composition, antioxidant activity, and gut microbiota associated with pumpkin juice fermented by *Rhodobacter sphaeroides*. Food Chem. 2022;401(4):134122.
24. Zhang L, Liu L, Wang KF, Xu L, Zhou L, Wang W, Li C, Xu Z, Shi T, Chen H, Li Y, Xu H, Yang X, Zhu Z, Chen B, Li D, Zhan G, Zhang SL, Zhang LX, Tan GY. Phosphate limitation increases coenzyme Q_{10} production in industrial *Rhodobacter sphaeroides* HY01. Synth Syst Biotechnol. 2019;4(4):212–9.
25. de Sena Aquino AC, Azevedo MS, Ribeiro DH, Costa AC, Amante ER. Validation of HPLC and CE methods for determination of organic acids in sour cassava starch wastewater. Food Chem. 2015;172:725–30.
26. Imam S, Yilmaz S, Sohmen U, Gorzalski AS, Reed JL, Noguera DR, Donohue TJ. iRsp1095: a genome-scale reconstruction of the *Rhodobacter sphaeroides* metabolic network. BMC Syst Biol. 2011;5(1):116.
27. Görlach A, Bertram K, Hudecova S, Krizanova O. Calcium and ROS: a mutual interplay. Redox Biol. 2015;6:260–71.

Publisher's Note